Optomechanical thermal intermodulation noise

S. A. Fedorov,[1,*] A. Beccari,[1,*] A. Arabmoheghi,[1] D. J. Wilson,[2] N. J. Engelsen,[1] and T. J. Kippenberg[1,†]

[1] *Institute of Physics (IPHYS), École Polytechnique Fédérale de Lausanne, 1015 Lausanne, Switzerland*
[2] *College of Optical Sciences, University of Arizona, Tucson, Arizona 85721, USA*

(Dated: February 23, 2020)

Thermal fluctuations give rise to a number of noise processes in optical interferometers, limiting the sensitivity of precision measurements ranging from the detection of gravitational waves to the stabilization of lasers for optical atomic clocks. In optical cavities, thermal fluctuations of length and refractive index result in cavity frequency noise, which can linearly couple to the optical field. Here we describe a different kind of noise process, thermal intermodulation noise, produced from the cavity frequency fluctuations by the inherent nonlinearity of optical susceptibility in laser-cavity detuning. We study thermal intermodulation noise due to the Brownian motion of membrane resonators in membrane-in-the-middle optomechanical cavities at room temperature, and show it to be the dominant source of classical intracavity intensity fluctuations under nearly-resonant optical excitation. We are able to operate at nominal quantum cooperativity equal to one an optomechanical cavity with optical finesse $\mathcal{F} = 1.5 \times 10^4$ and a low effective mass soft clamped membrane mode with $Q = 4. \times 10^7$ as a mechanical oscillator. In this regime, the magnitude of thermal intermodulation noise created by the mixing products of all membrane modes exceed the vacuum fluctuations by tens of decibel, preventing the observation of pondermotive squeezing. The described noise process is broadly relevant to optical cavities, in particular for which thermal frequency fluctuations are not negligible compared to the cavity linewidth.

I. INTRODUCTION

Optical cavities are ubiquitous in physical experiments. Their applications include precision interferometric position measurements, an extraordinary example of which is direct gravitational wave detection[1, 2], stable frequency references[ref], and quantum experiments, including cavity quantum electrodynamics[ref] and optiomechanics[3]. Optical cavities have finite temperature and therefore their frequencies exhibit fundamental thermal fluctuations due to the Brownian motion of mirror surfaces, thermorefractive and thermoelastic fluctuations[4, 5] and other processes that modulate the effective cavity length. These fluctuations predominantly manifest as excess phase noise in an optical field resonant with the cavity. At the same time, the nonlinearity of cavity discrimination curve creates intensity noise in the resonant field, which is especially pronounced when the magnitude of frequency fluctuations is comparable to the optical linewidth. This effect is known as intermodulation noise as it mixes different harmonics of the frequency noise. Technical intermodulation noise is known to limit the stability of frequency standards[6] and cavity-stabilized lasers[7, 8]. Here we report and study thermal intermodulation noise (TIN) of fundamental origin.

The transduction of optical path difference into measured signal in optical interferometers is periodic with the period equal to wavelength, λ, and therefore inherently nonlinear. Similarly, an optical cavity transduces the fluctuations of round-trip optical path, δx, to the modulation of intracavity field linearly only as far as the accumulated phase shift, $\delta\phi$, given by

$$\delta\phi = \mathcal{F}\delta x/\lambda, \tag{1}$$

is much smaller than one. Therefore high optical finesse not only increases the resolution of a cavity as an optical path sensor but also limits its dynamic range to $\lambda/\mathcal{F}$[9, 10]. This is a particularly important consideration in experiments in which, on one hand, high finesse is desirable to increase the strength of light-matter interaction, and, on the other hand, stringent constraints exist on the tolerable level of extraneous noise in both quadratures of the optical field. Experiments on quantum cavity optomechanics are among such.

Quantum cavity optomechanics studies aspects of interaction between optical field and mechanical motion such as position measurements and feedback control in presence of measurement-backaction[11, 12], the preparation of mechanical ground[13–15], single-phonon[16] and entangled[17] states and ponderomotive squeezing[18, 19]. In a handful of recent experiments, some quantum optomechanical effects were demonstrated at room temperature[20–24], limited due to high thermal noise levels. Most of these experiments[22–24] operated in an exotic regime when the radiation pressure spring exceeded the natural frequency of the mechanical oscillator by two orders of magnitude. An alternative platform which is considered promising for reaching the quantum regime of optomechanical interaction at room temperature is membrane in the middle system[25, 26]. It is predicted that quantum-backaction dominated regime is reacheable at microwatt input optical powers with the help of recently developed high-stress Si_3N_4 membrane resonators hosting high-Q and low mass soft-clamped modes[27, 28]. Yet, concomitant with this approach is a dense spectrum

* These authors contributed equally
† tobias.kippenberg@epfl.ch

of membrane modes that equally couple to the optical field and produce large thermal frequency fluctuations.

From the perspective of linear optomechanics, high temperature only requires increasing the input optical power to the point at which the optomechanical coupling rate compensates for the mechanical decoherence and the quantum cooperativity, C_q, reaches unity,

$$C_q = \frac{4g^2}{\kappa\Gamma_{\rm th}} \sim 1. \tag{2}$$

Here g is the loaded optomechanical coupling rate, κ is the optical linewidth and $\Gamma_{\rm th} = \Gamma_m n_{\rm th}$ is the mechanical thermal decoherence rate equal to the product of mechanical energy relaxation rate and phonon occupancy. If thermal intermodulation noise is taken into account, the effect of high temperature is more detrimental, as high absolute magnitude of Brownian motion produces strong extraneous classical noise. Unless the magnitude of intermodulation noise is smaller than the optical vacuum fluctuations, no quadrature of the optical field is quantum-limited.

The manuscript is structured as follows. In the beginning we introduce a theoretical model of thermal intermodulation noise due to the Brownian motion of mechanical resonator in an optomechanical cavity. Next we present measurements in low-cooperativity regime which reveal an extraneous intensity noise source in a resonantly driven membrane-in-the-middle cavity. We show the noise to match the expected from the model magnitude and scaling with optical linewidth. Finally, employing a PnC membrane with a low effective mass soft clamped mode we conduct measurements the regime $C_q \sim 1$, and study the dependence of TIN on laser detuning, and find it to be in excellent agreement with our theoretical prediction. Moreover, we show that the intermodulation noise poses a significant limitation for the observability of quantum backaction-imprecision correlations in such system.

[Mention in the introduction the relation to quadratic optomechanical transduction]

II. THEORY OF INTERMODULATION NOISE

We begin by presenting the theory of thermal intermodulation noise in an optical cavity under the assumption that the frequency fluctuations are slow compared to the optical decay rate. We concentrate on the lowest-order, i.e. quadratic, nonlinearity of the cavity detuning transduction.

Consider an optical cavity with two-ports which is driven by a laser coupled to port one and the output from port two of which is directly detected on a photodiode. In the classical regime, i.e. neglecting vacuum fluctuations, the intracavity optical field, a, and the output field

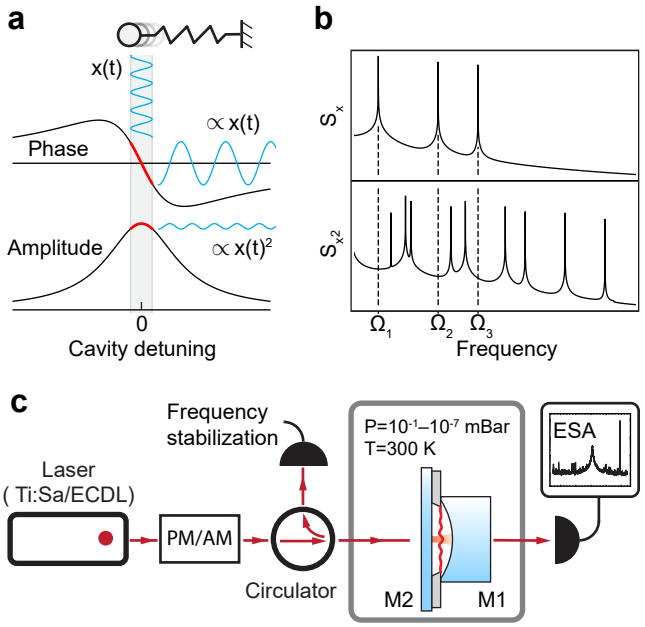

FIG. 1. a) Transduction of the oscillator motion to the phase (upper panel) and amplitude (lower panel) of resonant intracavity light. b) Spectra of linear (upper panel) and quadratic (lower panel) position fluctuations of a multimode system. c) Experimental setup.

$s_{\rm out,2}$ are found from the equations

$$\frac{da(t)}{dt} = \left(i\Delta(t) - \frac{\kappa}{2}\right) a(t) + \sqrt{\kappa_1}\, s_{\rm in,1}, \tag{3}$$

$$s_{\rm out,2}(t) = -\sqrt{\kappa_2} a(t). \tag{4}$$

where $s_{\rm in,1}$ is the constant coherent drive amplitude, $\Delta(t) = \omega_L - \omega_c(t)$ is the detuning from the cavity resonance, modulated by the cavity frequency noise, and $\kappa_{1,2}$ are the coupling rates of the ports one and two. Observe that it follows from Eq. 4 that the intensity of the detected light is directly proportional to the intracavity intensity. In the fast cavity limit, when the optical field adiabatically follows $\Delta(t)$, the intracavity field is found as

$$a(t) = 2\sqrt{\frac{\eta_1}{\kappa}} L(\nu(t))\, s_{\rm in,1}, \tag{5}$$

where we introduced for brevity the normalized detuning $\nu = 2\Delta/\kappa$, the cavity decay ratios $\eta_{1,2} = \kappa_{1,2}/\kappa$ and Lorentzian susceptibility

$$L(\nu) = \frac{1}{1 - i\nu}. \tag{6}$$

Expanding L in Eq. 5 over small detuning fluctuations $\delta\nu$ around the mean value ν_0 up to the second order we find the intracavity field as

$$a = 2\sqrt{\frac{\eta_1}{\kappa}} L(\nu_0)(1 + iL(\nu_0)\delta\nu - L(\nu_0)^2\delta\nu^2) s_{\rm in,1}. \tag{7}$$

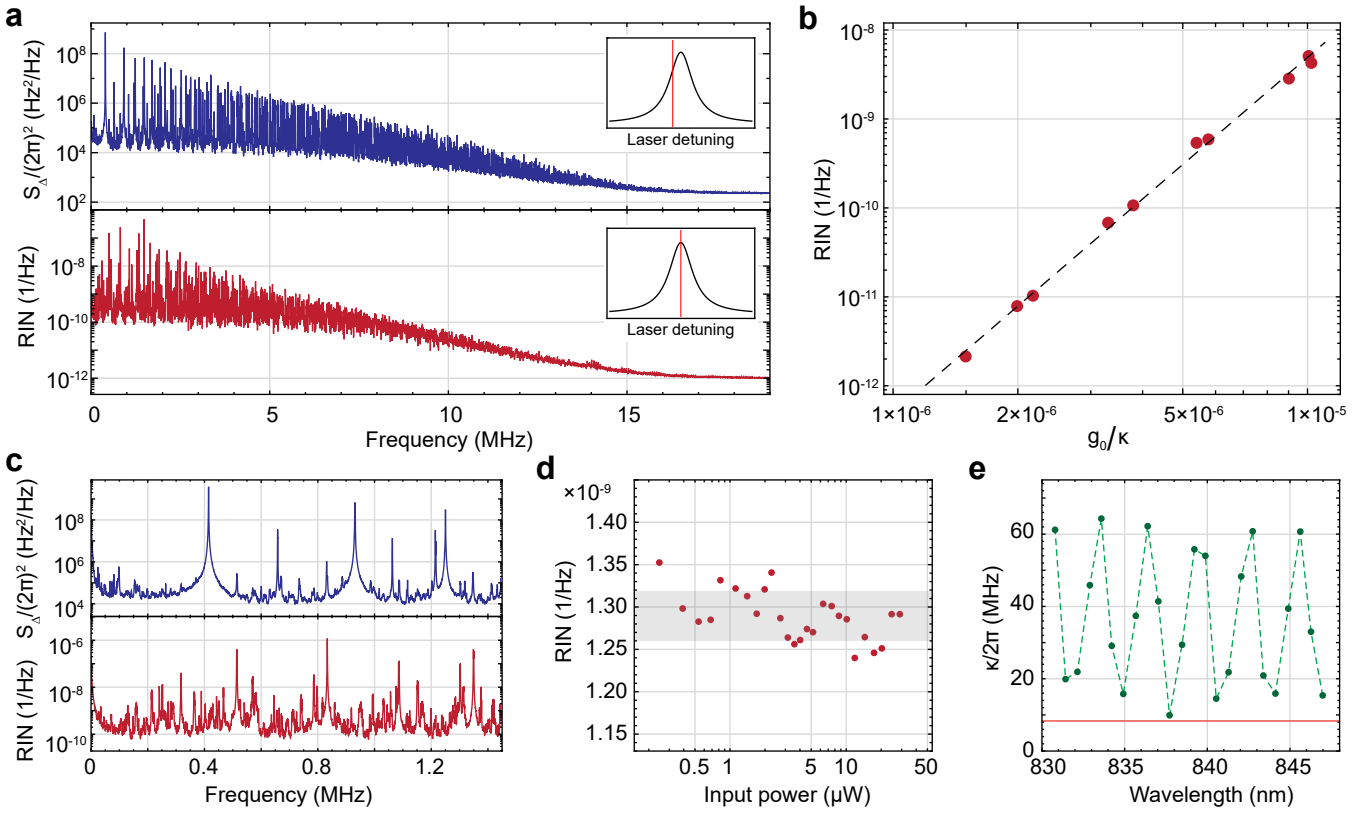

FIG. 2. a) Noise from a MIM cavity with laser detuned from resonance and on resonance. 1 mm square membrane, $\kappa/2\pi = 26.6$ MHz, $g_0/2\pi = 330$ Hz. c) The low frequency part of data in a). b), d) and e) show measurements for MIM cavity with 2 mm square membrane. b) dependence of the average RIN in $0.6-1.6$ MHz band. b) Power sweep on the resonance with wavelength 837.7 nm, band $\pm$ one standard deviation around the mean is shaded gray. e) Green points — measured linewidths of different optical resonances of MIM cavity, the dashed line is a guide to eye. Orange line — linewidth of an empty cavity with the same length.

According to Eq. 7, the intracavity field is modulated by the cavity frequency excursion, $\delta\nu$, and the frequency excursions squared, $\delta\nu^2$. If $\delta\nu(t)$ is a stationary Gaussian noise process, like a thermal noise, the linear and quadratic contributions are uncorrelated (despite clearly not being independent). This is due to the fact that odd-order correlations vanish for Gaussian noise,

$$\langle \delta\nu(t)^2 \delta\nu(t+\tau)\rangle = 0, \tag{8}$$

where $\langle ...\rangle$ is time-average, for arbitrary time delay τ.

Next, we consider the ptotodetected signal, which, up to an unimportant conversion factor, equals to the intensity of the output light and found as

$$I(t) = |s_{\mathrm{out},2}(t)|^2 \propto |L(\nu_0)|^2 \left(1 - \frac{2\nu_0}{1+\nu_0^2}\delta\nu(t) + \frac{3\nu_0^2-1}{(1+\nu_0^2)^2}\delta\nu(t)^2\right). \tag{9}$$

Notice, that there exist "magic" detunings, $\nu_0 = \pm 1/\sqrt{3}$, at which quadratic frequency fluctuations do not contribute to the detected signal and the intermodulation noise vanishes to the leading order.

The spectrum of the detected signal is an incoherent sum of linear term,

$$S_{\nu\nu}[\omega] = \int_{-\infty}^{\infty} \langle \delta\nu(t)\delta\nu(t+\tau)\rangle e^{i\omega\tau} d\tau, \tag{10}$$

and quadratic term, which for Gaussian noise can be found using the Wick's theorem[29]

$$\langle \delta\nu(t)^2 \delta\nu(t+\tau)^2\rangle = \langle \delta\nu(t)^2\rangle^2 + 2\langle \delta\nu(t)\delta\nu(t+\tau)\rangle^2, \tag{11}$$

as

$$S_{\nu\nu,2}[\omega] = \int_{-\infty}^{\infty} \langle \delta\nu(t)^2\delta\nu(t+\tau)^2\rangle e^{i\omega\tau} d\tau = 2\pi\langle\delta\nu^2\rangle^2\delta[\omega] + 2\times\frac{1}{2\pi}\int_{-\infty}^{\infty} S_{\nu\nu}[\omega']S_{\nu\nu}[\omega-\omega']d\omega', \tag{12}$$

where δ is delta-function.

III. THERMOMECHANICAL INTERMODULATION NOISE

In an optomechanical cavity the dominant source of cavity frequency fluctuations is the Brownian motion of mechanical modes coupled to the cavity,

$$\delta\nu(t) = 2\frac{G}{\kappa}x(t), \tag{13}$$

where $G = -\partial\omega_c/\partial x$ is the linear optomechanical coupling constant, and x is the total membrane displacement, the sum of independent contributions x_n of different mechanical modes. The spectrum of Brownian frequency noise is found as

$$S_{\nu\nu}[\omega] = G^2 \sum_n S_{xx,n}[\omega], \tag{14}$$

where $S_{xx,n}[\omega]$ are the displacement spectra of individual membrane modes (see SI for more details). Applied to Eq. 14, the convolution in Eq. 12 produces noise peaks at sums and differences of mechanical resonance frequencies, together with broadband background due to off-resonant components of thermomechanical noise, which is illustrated in Fig. 1b.

[Introduce quantum optomechanical parameters]

For the following discussion of quantum optomechanical effects it is useful to introduce vacuum optomechanical coupling rate of an individual mode

$$g_0 = Gx_{\mathrm{zpf}}, \tag{15}$$

where $x_{\mathrm{zpf}} = \sqrt{\hbar/2m_{\mathrm{eff}}\Omega_m}$ is the magnitude of zero point fluctuations, Ω_m is the mechanical resonance frequency and m_{eff} is the effective mass.

The theory of Sec. II applies in this case at optical powers sufficiently low so that the radiation-pressure mediated driving of the mechanical modes by the intermodulation noise is negligible. If this condition is not satisfied, radiation-pressure correlations may make the spectrum more complex. [This is because the mechanical state becomes non-Gaussian[30]]

The nonlinearity of optical detuning transduction imprints on the optical field signal proportional to x^2 in way analogous, but not equivalent, to the nonlinear optomechanical coupling, $\partial^2\omega_c/\partial x^2$. This effect was studied previously[30–32]. Interestingly, it was observed[30] that the cavity transduction commonly results in nonlinearity that is orders of magnitude stronger than the highest experimentally reported $\partial^2\omega_c/\partial x^2$, when compared by the magnitude of the optical signal proportional to x^2. In the Supplementary Information it is shown that the same is true for membrane in the middle cavity, in which typical quadratic signals originating from the nonlinear transduction and leading to intermodulation noise are by the factor of $r\mathcal{F}$ (where r is membrane reflectivity) larger than the signals due to the nonlinear optomechanical coupling, $\partial^2\omega_c/\partial x^2$.

IV. EXPERIMENTAL OBSERVATION OF EXTRANEOUS AMPLITUDE NOISE

A startling manifestation of the optical transduction nonlinearity is the emergence of thermal amplitude noise in the field, output from an optomechanical cavity under resonant optical excitation. In the conventional picture of linear optomechanics, intensity fluctuations of the light that goes out of the cavity under such conditions is shot noise limited or contains a small portion of thermal signal transduced by dissipative coupling. In reality, however, the intensity of light can contain of vast amount of thermal intermodulation noise. We study this noise systematically with rectangular membranes in the low-cooperativity regime.

Our experimental setup consists of a membrane in the middle cavity, composed of two supermirrors with the transmission of 100 ppm and a 200 um-thick silicon chip sandwiched between them that hosts a suspended high-stress silicon nitride membrane (see Fig. 1c). The membrane in the middle cavity is situated in a vacuum chamber at room temperature, it is probed using the light form a Ti:Sa or a tunable ECDL laser with wavelength around 840 nm. The Ti:Sa laser is used for noise measurements, whereas the diode laser is used only for the characterization of optical linewidths. The light reflected from the cavity is used for PDH locking, whereas the light exiting the cavity from the second port and detected in direct detection constitutes our measurement signal.

While reaching the quatum regime of optomechnaical interaction requires engineering high-Q and low mass mechanical oscillators, we perform the characterization of thermal intermodulation noise in low-cooperativity regime using conventional 20 nm-thick square membranes. In order to eliminate the influence of dynamic backaction, while characterizing the noises we keep the residual pressure in the vacuum chamber high, in the range 0.22 ± 0.03 mBar, so that the quality factor of the fundamental membrane mode is gas-damping limited to $Q \sim 10^3$.

We start by presenting in Fig. 2a and c the observation of strong classical amplitude noise in the output from the cavity subjected to resonant optical excitation. For MIM cavity with 1mm $\times$ 1mm $\times$ 20nm membrane and the input power of 5 μW the classical amplitude noise rises above the shot noise level by about 25 dB at low frequencies. In Fig. 2a, the noise level approaches shot noise at high frequencies due to averaging of the membrane mode profiles of the cavity waist (approx 25 μm in our experiment).

Next we prove that the observed amplitude noise originates from the nonlinearity of cavity transduction by performing noise measurements across different optical resonances of the same cavity and referring the amplitude noise level to the value of vacuum optomechanical coupling rate of the fundamental mode over the optical linewidth (see Fig. 2b). We use a 2mm $\times$ 2mm $\times$ 20nm membrane for this measurement. While the power spectral density of linearly transduced thermal fluctua-

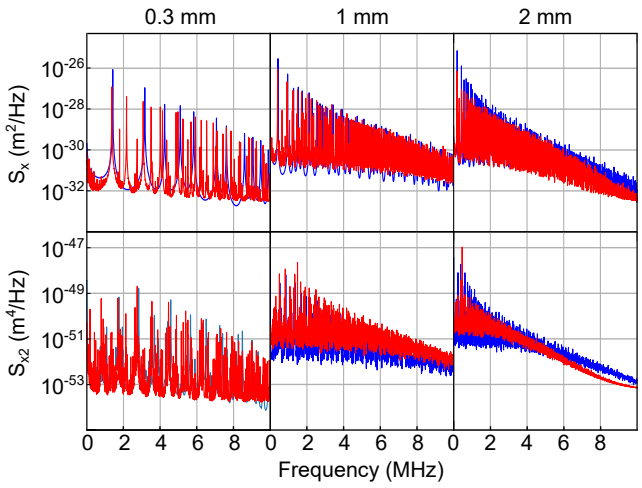

FIG. 3. Cavity-waist averaged position (top row) and position squared (bottom row) noises produced by the modes of 20-nm Si_3N_4 rectangular membranes of different sizes. Red is experimental data and blue is theoretical prediction. (Warning: two-sided theory spectra might be plotted, also the data for 2 mm membrane should be replaced) [also need to remove the cavity delay correction]

tions is $\propto (g_0/\kappa)^2$, the spectral density of quadratically transduced noise is $\propto (g_0/\kappa)^4$, a trend that is perfectly consistent with the data in Fig. 2b. By performing a sweep of the input laser power on one of the resonances (see Fig. 2d) we show that the intermodulation noise level is power-independent and therefore the observed noise is not related to the optomechanical dynamic backaction, negligible for the operation in low vacuum.

The intermodulation noise observed in our experiment is well reproduced by a theoretical model with no fitting parameters.

In our experiment the effect of finite cavity response time is small compared to the effect of geometric overlap, but we still take it into account. By using Eq. 9 and Eq. **??** we can find the spectrum of quadratically tansduced fluctuations and the resulting amplitude noise given the spectrum of cavity frequency fluctuations from Eq. 14. We present a comparison between experimentally measured linear and quadratic displacement noise spectra and the ones calculated using the theoretical model in Fig. 3. The inputs for the model in this case are experimentally measured g_0 of the fundamental membrane mode, the optical linewidth κ, the membrane size and its quality factors (for simplicity, assumed to be the same for all the modes). While our model is not detailed enough to reproduce precisely all the noise features, it well reproduces the overall level and the broadband envelope of the intermodulation noise that were observed in experiment.

[Mention that the laser locking does not affect the intermodulation noise]

[Add discussion that the potential dissipative coupling can only produce a much weaker effect on the intermodulation noise]

[Mention that Sxx are compared in Fig3 because these noises are intrinsic to membranes]

V. INTERMODULATION NOISE IN AN OPTOMECHANICAL CAVITY WITH A PHONONIC CRYSTAL MEMBRANE

The quantum regime of optomechanic interaction, when the radiation pressure shot noise matches the thermal force noise, is reached at the input laser power given by

$$P_{\rm in} = \frac{\pi c}{32\hbar}\frac{\lambda}{\mathcal{F}^2}\frac{S_{\rm FF,th}}{4r^2}, \tag{16}$$

where it is assumed that the membrane is positioned along the cavity to maximize the linear optomechanical coupling, λ is the optical wavelength, $\mathcal{F}$ is cavity finesse, r is membrane reflectivity and $S_{\rm FF,th}$ is the thermal force noise spectral density given by[33]

$$S_{\rm FF,th} = 2k_B T m_{\rm eff}\Gamma_m. \tag{17}$$

The reduction of thermal noise is essential for reaching the quantum backaction-dominated regime. Recently thermal noise down to 55 aN/$\sqrt{\rm Hz}$ was demonstrated at room temperature for soft-clamped modes localized in stressed phononic crystal membrane nanoresonators[27, 28], owing to the simultaneous enhancement of quality factor and the reduction of effective mass. Although similar force noise levels are attainable with trampoline resonators[34], the advantage of soft-clamped localized modes is their high frequency, on the order of MHz, which makes them less affected by classical laser noises. Even lower thermal noise, down to 10 aN/$\sqrt{\rm Hz}$, was demonstrated for soft-clamped modes in nanobeam[35] resonators, but nanobeams are not straightforward to combine with Fabry-Perot cavities.

The integration of a membrane resonator with a Fabry-Perot optical cavity generally involves tradeoffs for the attainable thermal noise. Practical constraints need have to be satisfied include maintaining a good overlap between the mechanical mode and the optical cavity waist and ensuring that the mechanical mode of interest is spectrally well isolated from other membrane modes.

In Fig. 4a and b we present designs of PnC membranes with defects optimized to create low effective mass and high-Q soft-clamped modes. The phononic crystal is made by a hexagon pattern of circular holes, which was introduced in Ref. [27] and makes the simplest arrangement that creates a complete phononic bandgap for the flexural modes. The phononic crystal is terminated to the frame at half the hole radii, which is necessary to avoid the appearance of modes, localized at the membrane edges—such modes have frequencies withing the phononic bandgap and can contaminate the mechanical spectrum.

Fig. 4a shows the microscope image of a resonator with trampoline defect, featuring a particularly low $m_{\rm eff} = 1.9$

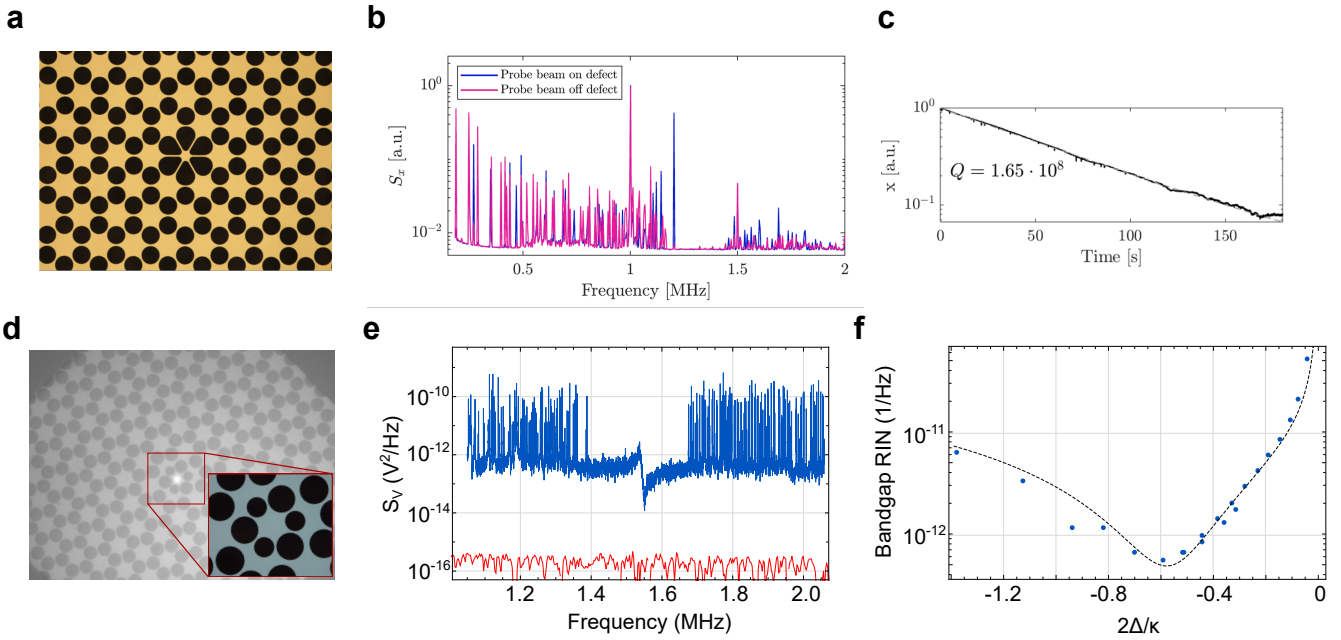

FIG. 4. a) Microscope image of a 3.6mm ×3.3mm × 20nm, with a low m_{eff} localized mode frequency of approximately 800 kHz, b) displacement spectrum of the membrane in a(replace data for this to be true) c) ringdown measurement of quality factor of the membrane in a. d) Microscope image of a 2mm × 2mm × 20nm membrane hosting a soft clamped mode. e) Blue—protocurrent noise spectrum detected with laser detuned from the cavity resonance, red—shot noise level. f) The variation of the relative intensity noise of the light output from MIM cavity at bandgap frequencies with laser-cavity detuning. Blue dots are experimental points, dashed line - single-parameter model fit.

ng at $\Omega_m/2\pi = 0.853$ kHz and $Q = 1.65\times10^8$, corresponding to the force noise of $S_{\text{FF,th}} = 15$ aN/$\sqrt{\text{Hz}}$. Another design, shown in Fig. 4d, is a 2 mm by 2 mm by 40 nm phononic crystal membrane with defect in the center that was engineered to create a single mode localized in the middle of phononic bandgap. This design features $Q = 4.1 \times 10^7$ at 1.5 MHz and the effective mass of 2.2 ng, which results in predicted $S_{\text{FF,th}} = 200$ aN/$\sqrt{\text{Hz}}$. The overall membrane size in this case of the second design is kept small enough so that no other modes, including in-plane ones, fall into the phononic bandgap. The complete membrane designs is available from Zenodo repository[36].

Using the membrane shown in Fig. 4d we were able to reproducibly assemble membrane-in-the-middle cavities with single-photon cooperativity $C_0 = 0.1 - 1$ (when operated in high vacuum, around 4×10^{-7} mBar in our case) and round trip loss lower than 200 ppm. According to the estimate provided by Eq. 16, in such cavities the quantum backaction-dominated regime is expected to be reached at the input powers of a few hundreds of μW. Our experiment, however, shows that at these powers the optical amplitude noise in such cavities is far from being limited by the vacuum fluctuations of light due to the intermodulation noise. The latter is big challenge for the exploration of quantum aspects of radiation pressure interaction at room temperature.

Fig. 4e shows the spectrum of light output from a membrane in the middle cavity with length around 350 μm, $g_0/2\pi = 360$ Hz, $\kappa/2\pi = 24.8$ MHz and the intrinsic loss rate around 100 ppm, close to the output coupling rate from the two cavity mirrors having the transmission of 100 ppm each. The laser was detuned to the red from the cavity resonance in this measurement, and the spectrum of output fluctuations contains both the contribution of thermomechanical noise linearly transduced by the cavity detuning and the intermodulation noise due to the nonlinearity in G/κ. In particular, at frequencies within the phononic bandgap the noise level is dominated by the intermodulation noise, which rises almost 40 dB above the level of vacuum fluctuations (calibrated separately by directing an auxiliary laser beam of the the same power on the detector). The intermodulation origin of the noise in the bandgap can be proven by considering the variation of the noise level with laser detuning presented in Fig. 4f. The laser power in this measurement was kept fixed to 30 μW, the cavity resonance wavelength is 840.1 nm.

We can understand the data in Fig. 4f using the general formula for the photocurrent produced in the detection of outgoing light (Eq. 9). Linear and quadratic position fluctuations are transduced differently by the cavity, but almost within the entire range of the detunings the quadratically transduced fluctuations dominate. The exception is the vicinity of the detuning $\Delta = \kappa/(2\sqrt{3})$ at which the quadratic transduction by the cavity is compensated by the quadratic transduction by the nonlinearity of photodetection (see SI for discussion). At this detuning the in-bandgap noise level is consistent with the mirror noise.

The overall variation of noise with the detuning can be described by the formula

$$S_{\mathrm{RIN}} \propto \frac{4\nu_0^2}{(1+\nu_0^2)^2} S_1 + \frac{1}{\nu_0}\frac{(3\nu_0^2-1)^2}{1+\nu_0^2} S_2, \qquad (18)$$

where S_1 is the contribution of mirror noise, which is independently calibrated, and S_2 is the contribution of quadratic noise that we use as a fitting parameter for the dashed curve in Fig. 4f. Aside from the cavity transduction, Eq. 18 takes into account the laser cooling of mechanical modes by dynamic backaction (assuming that the optical damping is much larger than the intrinsic linewidth, see SI for details). As can be seen from Fig. 4f, Eq. 18 very well reproduces the experimental data.

VI. CONCLUSIONS AND OUTLOOK

The suppression of intermodulation noise can be done by engineering mechanical resonators with lower multi-mode thermal noise and fewer modes, or by using optomechanical cavities with lower g_0/κ.

As a potential way to suppress the intermodulation noise we may suggest engineering the optical susceptibility in a way that the quadratic transduction vanishes, for example, using double resonance.

VII. ACKNOWLEDGEMENTS

This work was supported by...

[1] LIGO Scientific Collaboration, Classical and Quantum Gravity **32**, 074001 (2015).
[2] LIGO Scientific Collaboration and Virgo Collaboration, Physical Review Letters **116**, 061102 (2016).
[3] M. Aspelmeyer, T. J. Kippenberg, and F. Marquardt, Reviews of Modern Physics **86**, 1391 (2014).
[4] V. B. Braginsky, M. L. Gorodetsky, and S. P. Vyatchanin, Physics Letters A **271**, 303 (2000).
[5] M. L. Gorodetsky, Physics Letters A **372**, 6813 (2008).
[6] C. Audoin, V. Candelier, and N. Diamarcq, IEEE Transactions on Instrumentation and Measurement **40**, 121 (1991).
[7] B. A. Ferguson and D. S. Elliott, Physical Review A **41**, 6183 (1990).
[8] M. Bahoura and A. Clairon, IEEE Transactions on Ultrasonics, Ferroelectrics, and Frequency Control **50**, 1414 (2003).
[9] H. Miao, S. Danilishin, T. Corbitt, and Y. Chen, Physical Review Letters **103**, 100402 (2009).
[10] F. Khalili, S. Danilishin, H. Miao, H. Mller-Ebhardt, H. Yang, and Y. Chen, Physical Review Letters **105**, 070403 (2010).
[11] V. Sudhir, D. Wilson, R. Schilling, H. Schtz, S. Fedorov, A. Ghadimi, A. Nunnenkamp, and T. Kippenberg, Physical Review X **7**, 011001 (2017).
[12] D. J. Wilson, V. Sudhir, N. Piro, R. Schilling, A. Ghadimi, and T. J. Kippenberg, Nature **524**, 325 (2015).
[13] J. Chan, T. P. M. Alegre, A. H. Safavi-Naeini, J. T. Hill, A. Krause, S. Grblacher, M. Aspelmeyer, and O. Painter, Nature **478**, 89 (2011).
[14] L. Qiu, I. Shomroni, P. Seidler, and T. J. Kippenberg, arXiv:1903.10242 [quant-ph] (2019), arXiv: 1903.10242.
[15] M. Rossi, D. Mason, J. Chen, Y. Tsaturyan, and A. Schliesser, Nature **563**, 53 (2018).
[16] S. Hong, R. Riedinger, I. Marinkovi, A. Wallucks, S. G. Hofer, R. A. Norte, M. Aspelmeyer, and S. Grblacher, Science (2017), 10.1126/science.aan7939.
[17] R. Riedinger, A. Wallucks, I. Marinkovi, C. Lschnauer, M. Aspelmeyer, S. Hong, and S. Grblacher, Nature **556**, 473 (2018).
[18] A. H. Safavi-Naeini, S. Grblacher, J. T. Hill, J. Chan, M. Aspelmeyer, and O. Painter, Nature **500**, 185 (2013).
[19] T. P. Purdy, P.-L. Yu, R. W. Peterson, N. S. Kampel, and C. A. Regal, Physical Review X **3** (2013), 10.1103/PhysRevX.3.031012.
[20] T. P. Purdy, K. E. Grutter, K. Srinivasan, and J. M. Taylor, arXiv:1605.05664 [cond-mat, physics:physics, physics:quant-ph] (2016), arXiv: 1605.05664.
[21] V. Sudhir, R. Schilling, S. Fedorov, H. Schtz, D. Wilson, and T. Kippenberg, Physical Review X **7**, 031055 (2017).
[22] J. Cripe, N. Aggarwal, R. Lanza, A. Libson, R. Singh, P. Heu, D. Follman, G. D. Cole, N. Mavalvala, and T. Corbitt, Nature **568**, 364 (2019).
[23] M. J. Yap, J. Cripe, G. L. Mansell, T. G. McRae, R. L. Ward, B. J. J. Slagmolen, P. Heu, D. Follman, G. D. Cole, T. Corbitt, and D. E. McClelland, Nature Photonics , 1 (2019).
[24] N. Aggarwal, T. Cullen, J. Cripe, G. D. Cole, R. Lanza, A. Libson, D. Follman, P. Heu, T. Corbitt, and N. Mavalvala, arXiv:1812.09942 [physics, physics:quant-ph] (2018), arXiv: 1812.09942.
[25] J. D. Thompson, B. M. Zwickl, A. M. Jayich, F. Marquardt, S. M. Girvin, and J. G. E. Harris, Nature **452**, 72 (2008).
[26] D. J. Wilson, C. A. Regal, S. B. Papp, and H. J. Kimble, Physical Review Letters **103**, 207204 (2009).
[27] Y. Tsaturyan, A. Barg, E. S. Polzik, and A. Schliesser, Nature Nanotechnology **12**, 776 (2017).
[28] C. Reetz, R. Fischer, G. Assumpo, D. McNally, P. Burns, J. Sankey, and C. Regal, Physical Review Applied **12**, 044027 (2019).
[29] C. W. Gardiner, *Handbook of Stochastic Methods*, 2nd ed. (Springer, Berlin) section 2.8.1.

[30] G. A. Brawley, M. R. Vanner, P. E. Larsen, S. Schmid, A. Boisen, and W. P. Bowen, Nature Communications **7**, 10988 (2016).
[31] R. Leijssen, G. R. L. Gala, L. Freisem, J. T. Muhonen, and E. Verhagen, Nature Communications **8**, 1 (2017).
[32] A. B. Matsko and S. P. Vyatchanin, Physical Review A **97**, 053824 (2018).
[33] P. R. Saulson, Physical Review D **42**, 2437 (1990).
[34] C. Reinhardt, T. Mller, A. Bourassa, and J. C. Sankey, Physical Review X **6**, 021001 (2016).
[35] A. H. Ghadimi, S. A. Fedorov, N. J. Engelsen, M. J. Bereyhi, R. Schilling, D. J. Wilson, and T. J. Kippenberg, Science **360**, 764 (2018).
[36] Raw measurements data, analysis code to repoduce the manuscript figures, and the GDS designs of PnC membranes are available on zenodo.org, DOI:.../zenodo....